High-resolution facies zonation within a cold-water coral mound: the case of the Piddington Mound, Porcupine Seabight, NE Atlantic

*Aaron Lim** [1)], *Andrew J. Wheeler* [1) 2)] *and Aurélien Arnaubec* [3)]

[1)] *School of Biological, Earth and Environmental Sciences, University College Cork, Distillery Fields, North Mall, Cork, Ireland*

[2)] *Irish Centre for Research in Applied Geosciences, University College Cork, Ireland*

[3)]*Unité Systèmes sous-Marins, Centre de Méditerranée, Ifremer, Zone Portuaire de Brégaillon, CS 20330, 83507 La Seyne/Mer Cedex, France*

Abstract

Framework-forming cold-water corals (CWC's) such as *Lophelia pertusa* and *Madrepora oculata* generate positive topographic features on the seabed called CWC mounds. In the North East Atlantic, CWC mounds have been studied in detail and reveal heterogeneous spatial on-mound organisation of coral patches. Many of these studies are limited by a paucity of remotely-sensed and video imagery at an appropriate resolution and coverage. This study is the first attempt to video mosaic an entire CWC mound (the Piddington Mound of the Moira Mounds, Porcupine Seabight, Irish margin). The mosaic is divided into 18,980 0.25 m^2 cells with a manual classification applied to each within a geographic information system (GIS). Geospatial analysis shows that cell distribution is not random but clustered significantly across the mound surface. These clusters of cells make up a ring-like facies pattern. A model for the processes that lead to this facies pattern is suggested based on contemporary environmental

controls. Parallels to shallow-water reef atolls are also drawn which subsequently has implications for interpreting fossil coral outcrops.

*Corresponding author: aaron.lim@ucc.ie

Keywords: cold-water coral, habitat mapping, spatial analysis, sediments, facies distribution

1. Introduction

Framework-forming, scleractinian cold-water corals (CWCs) are sessile, filter-feeding organisms that can baffle current-suspended sediment and biogenic material between their framework (Roberts *et al.*, 2006). *Lophelia pertusa*, the most common framework-forming CWC in the NE Atlantic, has been found as shallow as 39 m water depth and as deep as 4000 m water depth (Freiwald *et al.*, 2004; Roberts *et al.*, 2006). In general, it occurs in temperatures between 4 and 13°C (Freiwald, 2002) and has proven to be tolerant of a wide range of salinities, from 31.7 - 38.8 ‰ (Davies *et al.*, 2008). As the coral framework grows, it baffles sediment which can help to generate topographic features on the seabed called CWC reefs and, through successive periods of reef development, CWC carbonate mounds (Freiwald, 2002; Roberts *et al.*, 2009). Here, we refer to mound-shaped, positive topographic features developed by CWC's as CWC mounds. CWC mounds are common in the NE Atlantic (Wheeler *et al.*, 2007), specifically where internal waves concentrate food particles (phytodetritus) which is delivered to CWCs by enhanced bottom currents (Dullo *et al.*, 2008; Mienis *et al.*, 2009; White and Dorschel, 2010).

Habitat mapping has proved to be a valuable, efficient and cost-effective tool in understanding the marine environment (e.g. Huang *et al.*, 2011; Lamarche *et al.*, 2011) including CWC habitats (Savini *et al.*, 2014). Multibeam Echosounder (MBES) bathymetry and backscatter have been used extensively to characterise current dynamics and their influence on CWC mound morphology and development e.g. in the straits of Florida, W Atlantic (Correa *et al.*, 2012a; Correa *et al.*, 2012b) and the midslope Moira Mounds, Porcupine Seabight, NE Atlantic (Foubert *et al.*, 2011). Recently, more advanced approaches to MBES surveying have imaged CWC habitats in deep water using ROV-borne MBES (Dolan *et al.*, 2008; Foubert *et al.*, 2011), on submarine terraces using AUV-borne MBES (Correa *et al.*, 2012a) and on vertical cliff faces in submarine canyons using forward-facing ROV-borne MBES (Huvenne *et al.*, 2011).

In the absence of adequate multibeam data, other studies (e.g. Dorschel *et al.*, 2007; Wheeler *et al.*, 2008) avail of current data, sediment types, video data and/or side scan sonar (SSS) surveying integrated within a Geographical Information System (GIS) to highlight the role of currents and sediment supply on CWC reefs and mounds. Seabed sediment samples are an effective way of studying CWC reefs although limited by the spatial representation of the sample (e.g. Day grab, <0.5 m^2). Video surveys can discriminate the seabed across substantial areas and are widely used in CWC habitat inspections (Foubert *et al.*, 2005; Huvenne *et al.*, 2005; Vertino *et al.*, 2010). Recent advances in underwater imaging have made high-resolution underwater imagery with accurate positioning in deep water environments possible (Kocak and Caimi, 2005). As a result, since 2005, the utilisation of ROV-based observations for facies information from CWC mounds has increased dramatically (e.g. De Mol *et al.*, 2007; Foubert *et al.*, 2008; Guinan *et al.*, 2009; Hebbeln *et al.*, 2014; Heindel *et al.*, 2010; Huvenne *et al.*, 2016; Purser, 2015; Wienberg *et al.*, 2013). Huvenne *et al.* (2005) demonstrate the variability between entire mound provinces along the Irish Margin highlighting both the frequency and variability of CWC mounds within the Belgica Mound Province. Later, Dorschel *et al.* (2007)

observed a correlation between living coral and enhanced bottom currents in the Belgica Mound Province and outlined the influence of contour currents, tidal currents and local topography on the distinct coral facies distribution across the Galway Mound. Results from other ROV-based facies mapping also highlight the strong relationship between local currents and facies distribution across a mound surface. For example, at the Franken Mound, a CWC mound in a state of "mound retirement" at the western Rockall Bank, shows a distinct facies distribution across the mound with living coral dominating the summit region (Wienberg *et al.*, 2008). Many other uses for ROV-based facies observations were realised. Heindel *et al.* (2010) test, for the first time, a method of spatial prediction mapping (maximum likelihood classification) on a CWC ecosystem providing detailed aerial estimates of CWC-typical facies. ROV-based facies observations were utilised to show that *L. petusa* is restricted to longer term, stable conditions while *M. occulata* is more tolerant towards environmental fluctuations (Wienberg *et al.*, 2009). Furthermore, its need as a tool in marine reserve designation and implementation is now recognised (Roberts *et al.*, 2005).

In addition, advances in image processing has led to the application of video mosaicking to marine habitat mapping (Rzhanov *et al.*, 2000). For example, Lirman *et al.* (2007) accurately characterise a tropical coral reef in shallow water using an entire reef-scale video mosaic. However, no such study has been carried out on an entire CWC reef although small parts of CWC habitats have been manually photo mosaicked (Wheeler *et al.*, 2011).

The need for more local-scale studies and data sets of equal resolution have previously been highlighted (Dolan *et al.*, 2008). This study presents the first attempt of video mosaicking an entire cold-water coral reef and subsequent analyses providing an in-depth facies mapping exercise allowing to discuss facies organisation and potential facies organisational influences.

1.1 Study Site

The Belgica Mound Province (BMP), partly enclosed with a Special Area of Conservation (SAC) designated under the EU Habitats Directive, is located on the eastern flank of the Porcupine Seabight, NE Atlantic (see Fig. 1) (Beyer *et al.*, 2003; Dorschel *et al.*, 2007; Huvenne *et al.*, 2002). It contains an abundance of (giant) CWC carbonate mounds, including the well-studied Galway Mound, Thérèse Mound and Challenger Mound (De Mol *et al.*, 2007; Dorschel *et al.*, 2007; Eisele *et al.*, 2008; Huvenne *et al.*, 2009; Kano *et al.*, 2007; Thierens *et al.*, 2010; Titschack *et al.*, 2009; Wheeler *et al.*, 2005). Two distinct CWC carbonate mound chains have been identified, orientated roughly N-S (parallel to depth contours) (Wheeler *et al.*, 2005). Pre-existing bathymetry highlights their slight elongate to conical morphology and typical dimensions (approx. 1 km across and 100 m tall) (Beyer *et al.*, 2003). To the east, these large CWC mounds are enclosed by the continental shelf and to the west, the Arwen Channel runs through the BMP (Murphy and Wheeler, 2017; Van Rooij, 2004). Towards the south and south-west, the Porcupine Seabight exits out to the abyssal plain (Dorschel *et al.*, 2010) while the north shallows to 500 m, outside the typical depth range for CWC growth on the Irish continental margin (Dullo *et al.*, 2008; White and Dorschel, 2010)

The Moira Mounds are small-type CWC reefs (approx. 30 m across and 10 m tall) found throughout the BMP, occurring between 800 - 1100 m water depth (Wheeler *et al.*, 2005). While no definitive dating has confirmed their age, it is speculated that they are Holocene features based on their size, seismic profiles and the surrounding seabed substrate (Foubert *et al.*, 2011; Huvenne *et al.*, 2005; Kozachenko, 2005). The Moira Mounds in the BMP can be further subdivided into 4 areas or chains of mounds based on the distribution of approx. 256 Moira Mounds; the “up-slope area”, the “mid-slope area”, the “down-slope area” and the “northern area” (Wheeler *et al.*, 2011) (see Fig. 1). While the number of Moira Mounds in the northern and the up-slope areas are relatively sparse, the main focus of research has been

carried out on the mid- and down-slope areas. The mid-slope area occurs between the chain of large CWC carbonate mound structures. The Moira Mounds here are thought to represent mound formation under "stressed" conditions due to high sediment input (Foubert *et al.*, 2011). The down-slope area is unique as it occurs within the Arwen Channel. Unlike the other areas, the CWC's on the Moira Mounds are predominantly growing, are actively trapping sands (Wheeler *et al.*, 2011) and occur outside the influence of other large mound structures.

<INSERT FIGURE 1>

2. Materials and Methods

2.1 ROV-borne Multibeam Echosounder (MBES)

ROV-borne MBES data was collected over the Piddington Mound and the surrounding seabed during the QuERCi survey (2015) on board *RV Celtic Explorer* with the *Holland 1 ROV* (cruise number CE15009: Wheeler *et al.* (2015). A high-resolution Kongsberg EM2040 MBES was integrated with a sound velocity probe and mounted on the front-bottom of the ROV. Data were acquired at a frequency of 400 kHz while the ROV maintained a height of 30 m above the seabed with a survey speed of approximately 2 knots. This achieved a swath width of ~ 160 m. Positioning and attitude were obtained using a Kongsberg HAINS inertial navigation system, ultra-short baseline (USBL) system (Sonardyne Ranger 2) and doppler velocity log (DVL). Data acquisition was carried out using SIS software, where calibration values, sensor offsets, navigation and attitude values were incorporated. Two adjacent 170 m long MBES lines were collected over Piddington Mound and the surrounding seabed. MBES data were stored as *.all and *.wcd files and were processed using CARIS HIPS and SIPS v9.0.14 to apply tidal corrections and clean anomalous data spikes. The cleaned data were saved as a single *.xyz and gridded to a 10 cm ArcView GRID.

143 The 10 cm MBES grid was imported into ArcMap 10.2 and projected in UTM Zone 29N. A 1
144 m contour *.shp file was generated using the Arc Toolbox Spatial Analyst Contour tool. Slope
145 (degrees) and aspect were derived from the bathymetry using the Arc Toolbox Spatial Analyst
146 tools.

147

148 2.2 ROV-video data collection

149 ROV-video data was collected over Piddington Mound during the VENTuRE survey (2011)
150 on board *RV Celtic Explorer* with the *Holland 1 ROV* (cruise number CE11009: Wheeler and
151 shipboard party, 2011). A downward-facing, high-definition camera was mounted on the
152 bottom of the ROV. Positioning and navigation were achieved using a USBL (Sonardyne
153 Ranger 2) and RDI Workhouse DVL. The ROV altimeter recorded and logged the height of
154 the ROV from the seabed. The ROV recorded downward-facing HD video during a series of
155 transects across the mound <2 m off the seabed/mound surface.

156

157 2.3 Georeferenced video mosaic generation

158 A georeferenced video mosaic has been generated using the IFREMER in-house *Matisse*
159 software where the raw video data was imported and from which images have been extracted
160 at a rate of 1 per second. Poor quality imagery, possibly due to an excessive fly height, and/or
161 with a poor navigational lock were not included. The associated USBL navigation has been
162 filtered with a sliding median filtering and 2^{nd} order polynomial model fit in order to lower
163 trajectory noise. Image and navigation data have been synchronized so that each image has an
164 initial approximate position. This position is refined later by the mosaicking process. For this
165 refinement, the first process consists of feature detection and matching between images using
166 the SIFT (Scale Invariant Feature Transform) algorithm (Lowe, 1999), known for its strong

167 robustness and accuracy. Image matching alone would lead to a drifting mosaic and invalid
168 scale, while USBL navigation alone is not accurate enough for high-quality local-overlapping
169 but gives accurate global positioning. To benefit from the both image matching and USBL-
170 navigation, we merged image and navigation information through a cost function
171 minimization. This developed method is similar to Ferrer *et al.* (2007) except cost function
172 weights are affected according to image and navigation data standard deviations so re-
173 projection errors are minimized in the mosaicking plane rather than the image plane.

174 After this step, image positions are refined and the mosaic can be drawn. This is carried out
175 with state of the art seaming and blending techniques after Burt and Adelson (1983) and Kwatra
176 *et al.* (2003).

177 2.4 Seabed classification

178 As the ROV could not be maintained at a constant height above the seabed in video surveying
179 mode in strong currents, seawater-induced blue-shift varied across the video mosaic. Hence,
180 neither a supervised nor an unsupervised (automatic) seabed classification could be utilized.
181 Instead, a manual classification was applied to each cell of the entire video mosaic. An ArcMap
182 fishnet with a cell size of 0.25 m^2 was overlaid on the video mosaic to manage the supervised
183 classification at the highest resolution possible where each 0.25 m^2 cell can be inspected and
184 classified (totally 18,980 cells).

185 Classifiers were based on preliminary assessment of the video mosaic and other CWC habitat
186 ROV-dive-based facies classification from previous work, some of which have similar
187 objectives or are proximal to the study site (e.g. Dorschel *et al.*, 2007; Dorschel *et al.*, 2009;
188 Douarin *et al.*, 2014; Heindel *et al.*, 2010; Huvenne *et al.*, 2005; Spezzaferri *et al.*, 2012;
189 Vertino *et al.*, 2010; Vertino *et al.*, 2015; Wheeler *et al.*, 2005; Wienberg *et al.*, 2008; Wienberg
190 *et al.*, 2009). The facies classifiers are: “hemipelagic sediment with dropstones”, “coral

191 rubble", "hemipelagic sediment", "dead coral framework" and "live coral framework" (see Fig.
192 2 for examples and results for detailed facies descriptions).

193 As each individual cell is inspected and a suitable class chosen, a value was assigned to an
194 attribute table. Several preliminary classifications were applied to the video mosaic in different
195 locations to test the individual classifiers and the classification itself. Some areas of the
196 preliminary classification were re-classified and compared to their initial classification to
197 ensure classification accuracy. The entire video mosaic was then classified and saved as a *.shp
198 file.

199

200 2.5 Video-mosaic analysis

201 Spatial dependency is measured by various spatial autocorrelation statistics (e.g. Moran's *I*:
202 Goodchild, 1986) . However, these are unrepresentative when spatial autocorrelation varies
203 significantly over the study site. More suitably, Anselin (1995) developed local indicators for
204 spatial association (LISA) which, in contrast to other methods, measures local variation within
205 patterns of spatial dependence that may not be represented in existing techniques. A widely-
206 used LISA is the *G* statistic (Getis and Ord, 1992; Ord and Getis, 1995). This measures how
207 concentrated high or low values are for a given study area by calculating a z-score (standard
208 score) and p-value (calculated probability) of a set of geographical values. Here, it is utilised
209 to measure the degree of clustering of the classified cells via the Arc Toolbox spatial statistics
210 tools (High/Low clustering Tool) based on Euclidean distances.

211 The classified *.shp file was converted to a raster using the conversion tools in Arc Toolbox
212 and imported to the Focal Statistics tool. This calculates, for each input cell location, a statistic
213 of the value that occurs most often (majority) within a specified neighbourhood around it. The

specified neighbour was calculated based on a potential navigational error of the ROV (<5 m). Therefore, the neighbourhood was defined as 2.5 m radius around each cell location.

3. Results

3.1 Video mosaic

The video mosaic was generated from approximately 8 hours of high-definition video data. The data was collected by means of a series of over lapping lines covering the mound and immediate off-mound area. The video mosaic is shown in Fig. 2, holes in the mosaic are a result of data rejection. For subsequent display purposes, colours on the mosaic were adjusted manually selecting both a white and black reference within Corel Draw software package.

<INSERT FIGURE 2>

3.2 Bathymetry and slope

Piddington Mound exists in an area with several other mounds (Fig. 3A). It has a similar size (11.8 m tall, 60 m x 40 m across) and morphology (slightly elongated conical) as the surrounding mounds and it has substantial scouring (1 m - 3 m deep) at its southern limit. Sinuous megaripples (sediment waves) exist across the area around these mounds. They have a wavelength of ~10 m and a wave height of 20 cm – 75 cm. To the south of each mound, there are positive, ridge-shaped features 0.5 m - 2 m tall. These features are unlike the sediment waves as they are larger than the sediment waves, have coral colonising them and biogenic material deposited in their troughs as shown by the oblique video footage (Fig. 4). These ridge and wave features are not included in the facies classification as they are not on the Piddington Mound or in the immediate environment and therefore not covered by the video mosaic.

<INSERT FIGURE 3>

<INSERT FIGURE 4>

The deep blue colour represents flat seabed slopes (minimum slope of 0°) while the red colour represents the steep seabed slopes (maximum slope of 55.7°), all relative to this data set (Fig. 3B). Note that regional slope angle in this area is 1.2º. The steepest areas are found on the flanks of the mounds with slopes dipping as steep as 55°. The summit of each mound is relatively flat (0-6°) as are areas away from the mounds (0° - 6°) (Fig. 3B). This figure also includes the slip faces of mega ripples in the areas away from the mounds. These appear sinuous to cuspate with a wavelength of 7 m - 10 m and wave height of 4 cm - 20 cm with an east-west crest alignment. The larger coral colonised ridge-shaped features (0.5 m - 2 m tall) south of the mounds are morphologically distinct, with short east-west aligned linear crests and a wavelength of approx. 10 m. They diminish in size away from the mounds.

3.3 Seabed classification

<INSERT FIGURE 5>

The "hemipelagic sediment with dropstones" class is characterised by the cell being dominated (>50 % cell coverage) by dropstones and sediment (sand or mud). This class occurs most commonly around the mound perimeter. The "coral rubble" class is characterised by a cell dominated (>50% cell coverage) by recognisable biogenic material (i.e. coral rubble, shell fragments) and sediment. This class most commonly occurs in a 10 m wide ring immediately enclosed by the "hemipelagic sediment with dropstones" class. However, minor occurrences of this class exist both to the centre of the mound and outside of this ring. This ring is elongate in the same direction of the current (N-S). The "hemipelagic sediment with dropstones" and "coral rubble" classes are the most frequent classified cells in the video mosaic (Fig.5). The "hemipelagic sediment" class is characterised by the cell being dominated (>90% cell

coverage) by hemipelagic sediment i.e. sand or mud with no recognisable bioclasts or dropstones. It is the least common class and occurs in small clusters less than 0.75 m wide typically around the edges of the "coral rubble" class. The "dead coral framework" class is characterised by the cell being dominated (>50% cell coverage) coral framework which has no identifiable living parts. This class occurs across the mound but is concentrated in the centre and southern central area as a North-South-elongate ring. The "live coral framework" class is characterised by the cell being dominated (>50% cell coverage) by coral framework with identifiable living parts (polyps or mucus-covered frameworks evident) although major proportions of the coral framework may be dead. It is found across the mound, but is concentrated in the northern central area.

3.4 Spatial statistical analysis

The High-Low Clustering (Getis-Ord General G) analysis indicates the concentration of clustering. It firstly applies a null hypothesis to determine if clustering occurs. In this case, with a large Z-score (168.89) and small p-value (<0.001), the null hypothesis can be rejected meaning that clustering occurs. A positive Z-score indicates that high-values (coral frameworks) cluster.

The majority value of cells in the specified neighbourhood (2.5 m radius) (Fig. 6) reveals 4 facies occurring in 5 areas: "Hemipelagic sediment and dropstone" facies, "Coral rubble" facies, "Dead coral framework" facies, and "Live coral framework" facies. This means that in these facies, a particular cell-type dominates, as shown by the focal statistic (majority) based on a 2.5 m radius. The distribution of these facies closely follows the distribution of observed common occurrence of the individual classified cells. These facies have a ring/annulus-like distribution.

The “Hemipelagic sediment and dropstone” facies exists in the outer rim of this ring/annulus shape. It is made up of 74.9% “hemipelagic sediment and dropstone” cells, 15.9% “coral rubble” cells, 2.3% “dead coral framework” cells, 1.6% “hemipelagic sediment” cells and 1.3% “live coral framework” cells (Fig. 6b).

Immediately inside the “Hemipelagic sediment with dropstone” facies, the “Coral rubble” facies exists. However, this facies also protrudes 11.5 m through this facies NW of the mound and exists on the highest point of the mound (at -968 m water depth) protruding 11.5 m towards the ENE. It is made up of 60.6% “coral rubble” cells, 16.5% “dead coral framework” cells, 6.9% “live coral framework” cells, 6.3% “hemipelagic sediment and dropstone” cells and 1.6% “hemipelagic sediment” cells (Fig. 6b).

The “Dead coral framework” facies exists immediately inside the main body of the “Coral rubble” facies ring. It has a U-shape where the centre of the “U” is broadly based around the highest point on the mound. This facies is made up of 53.1% “dead coral framework” cells, 24.3% “coral rubble” cells, 17.4% “live coral framework” cells, 0.6% “hemipelagic sediment” cells and 0.1% “hemipelagic sediment and dropstone” cells (Fig. 6b).

Finally, the “Live coral framework” facies occurs 4.8 m north of the highest point on the mound, where it completes the U-shape of the “Dead coral framework zone” to make a complete ring, encircling the central “Coral rubble” facies. This zone has an irregular morphology where the zone is intruded by minor occurrences of the “Dead coral framework” facies. It is made up of 47.8% “live coral framework” cells, 32.1% “dead coral framework” cells, 13.6% “coral rubble” cells, 0.2% “hemipelagic sediment” cells and 0% “hemipelagic sediment and dropstone” cells (Fig. 6b).

306 The “hemipelagic sediment” cells were not common enough in any neighbourhood (2.5 m) to
307 develop its own facies in the focal statistics tool. However, their distribution in relation to these
308 facies is noted.

309 <INSERT FIGURE 6>

310 **4. Discussion**

311 4.1 Local sedimentary environment

312 East-west orientated sediment waves surrounding Piddington Mound and its neighbouring
313 mounds suggest a high-energy, bottom current-influenced, sedimentary environment (Foubert
314 *et al.*, 2011). The cross-profile morphology (steepened lee slope) of the sediment waves suggest
315 a south to north prevailing current across the area (Fig. 3B). The current-orientated, elongate
316 morphology may be owed to the dominance of currents here. In fact, substantial scouring
317 around the base of the mounds (Fig. 3A) highlights the intensity of these currents. The larger
318 ridge-form features (see Fig. 3A) to the south of the mounds may no longer be active sediment
319 transport bedforms as the presence of coral on them suggest stability since the growth of the
320 corals seen on the surface (see Fig. 4). However, as the internal composition is unknown
321 nothing about their origin can be said with certainty. De Mol *et al.* (2007) and Wheeler et al.
322 (2007) describe similar coral-topped features at the base of the Thérèse Mound.

323

324 4.2 Piddington Mound spatial organisation

325 The off-mound area of the Moira Mounds has been previously described (see Foubert *et al.*,
326 2011; Wheeler *et al.*, 2005). Off-mound areas are typically less spatially heterogeneous than
327 the on-mound areas (e.g. Vertino *et al.*, 2010). The video mosaic covers the entire Piddington
328 Mound surface and the immediate off-mound area, allowing inclusion of the full-mound
329 surface in the analyses. Further, the chosen resolution of the analyses is both commensurate

with typical box core footprints used to study other CWC mounds and is of sufficient resolution to map facies change and distribution.

The G-statistic reveals that, despite the heterogeneous nature of the facies on Piddington Mound observed from the video mosaic at a 0.25 m^2 scale, there is a statistically significant clustered pattern. The focal statistics layer shows the geographic distribution of cell-type dominance (Fig. 6a). The ring-like pattern of these dominating cell-types is clearly focussed around the summit of Piddington Mound observed in the bathymetric data (Fig. 3A). This ring-like clustered pattern is made up of facies typical of CWC mounds ("Live coral framework", "Dead coral framework" and "Coral rubble"). Similar facies have been identified at the nearby Galway Mound (Dorschel *et al.*, 2007), other Moira Mounds (Foubert *et al.*, 2011; Wheeler *et al.*, 2005), Atlantis Mound and Yellow Chain at the Santa Maria di Leuca Coral Province in the Mediterranean (Vertino *et al.*, 2010), Franken Mound (Wienberg *et al.*, 2008), Propeller Mound (Heindel *et al.*, 2010) and various mound provinces within the Porcupine Seabight (Huvenne *et al.*, 2005). The distribution of these mound-typical facies closely follows the mound depth contours. Where the seabed becomes relatively flat, surrounding Piddington Mound (Fig. 3B), it is characterised by "Hemipelagic sediment with dropstones" facies which is the typical background facies present in the area (Foubert *et al.*, 2011). It is therefore likely that the on-mound facies distribution can be attributed to the presence of corals where each facies may represent the result of a dominant process or set of processes at that part of the mound. The "Live coral framework" area slightly to the north of the Piddington Mound summit is the area on the mound where coral growth dominates. The "Coral rubble" areas on the mound, found near the summit and on the fringes of the reef, represent the areas where notable accumulations of eroded (physical or biological) coral and other biogenic material has been deposited. The "Dead coral framework" area found mainly on the flanks of the reef and are typically found where the "Coral rubble" and "Live coral framework" intersect. This area

355 represents an area where live coral growth no longer dominates and older framework remains
356 exposed.

357

358 4.3 Influences on facies distribution

359 The “Hemipelagic sediment and dropstone” facies dominates around the Piddington Mound
360 within the surrounding scour pits (Fig. 3A). Initial deposition of this dropstone-rich layer and
361 posterior re-exposure by erosion is rather unlikely as coring and drilling attempts in the vicinity
362 of the Belgica Mound Province CWC mounds never observed such a layer (e.g. IODP 307
363 Expedition scientists, 2005). Alternatively, perhaps the dropstones were scattered in
364 hemipelagic sediment in which winnowing of this sediment up-concentrated the dropstones.
365 This would also explain the preferential occurrence of the hemipelagic sediment with dropstone
366 facies within the scour pit.

367 The “hemipelagic sediment” cell-type is uncommon, existing in very small patches scattered
368 across Piddington Mound. However, its distribution is noted (Fig. 5) occurring in 2 different
369 settings. The first setting is next to coral framework cell-types (“Dead coral framework” and
370 “Live coral framework”) where the coral frameworks may act as a physical barrier to erosion
371 for the already deposited sediment from a former lower hydrodynamic energy regime. The
372 second setting is at the boundary between the “hemipelagic sediment and dropstone” cell-types
373 and “coral rubble” cell-types in the current-facing (southern) side of the mound. This
374 deposition of “hemipelagic sediment” may be explained by a sudden change in seabed rugosity
375 slowing the current between these two cell-types, allowing the deposition of current-suspended
376 sediment.

377 Wilson (1979) proposes a ring-like CWC growth (Wilson Ring model), particularly focussed
378 around the coppice stage (*sensu* Squires, 1964). Wilson (1979) describe CWC reef

development in optimum conditions, with limited sediment supply, where autogenic (biogenic) processes dominate; an isolated colony grows and successive rings of coral debris and colonies develop around this initial point (colony). This forms a circular CWC coppice made up of alternating rings of colonies and debris where, presumably, the centre is older than the edges of the structure. However, at the reef-scale, this process of ring-like development seems rather unlikely.

<INSERT FIGURE 7>

A more likely explanation for the ring-like distribution of facies across the Piddington Mound is based on benthic environmental conditions. Currents are well-known to influence facies distribution across CWC mounds (Dorschel *et al.*, 2007). In fact, previous research show that even local-scale (bio)zonation may be primarily controlled by current flow over them (Messing *et al.*, 1990). Here, currents are considered as the dominant (allogenic) control on the distribution of facies across Piddington Mound. CWC's preferentially settle on elevated structures where they have access to faster flowing water and enhanced food supply, undiluted by benthic sediment transport processes (Freiwald, 2002; Roberts *et al.*, 2003; Roberts *et al.*, 2006). F1 and F2 (Figure 7) occur relatively high (several meters above the surrounding seabed) on the Piddington Mound. This is also the steepest part of the mound (45-50°) which may be a result of coral trapping sediment and generating topography (Wheeler *et al.*, 2005; Wheeler *et al.*, 2008). Such steepened slopes may cause biologically and physically eroded bioclasts to roll onto the flatter parts of the mound (predominately the downslope R2). Thus, F1 and F2 are likely the source of the bioclasts that make up the "Coral rubble" facies in R2. The central "Coral rubble" facies at the mound summit (R1) occurs upslope and sheltered by a ring of coral framework and therefore its distribution cannot be explained by the same process. Here, this central area is fully encircled by dense coral framework which locally cuts it off from surrounding currents and subsequent food supply. Despite its elevated occurrence, a reduction

404 in food supply and current velocity may result in a less favourable environment at this central
405 area. This may explain the degradation of these corals to become an area of coral rubble. As
406 such, 3 comparisons can be drawn between Piddington Mound and shallow-water reef atolls
407 where a) a ring of coral shelters/cuts off the centre, creating a micro-environment, markedly
408 different from the surrounding environment akin to the central lagoon area of a shallow-water
409 reef atoll, b) the slope of the Piddington Mound is similar to that of shallow-water reef atolls
410 (45°) (e.g. Mururoa Atoll) (Chevalier, 1968) and subsequently c) the reef material is
411 transported down its slope (Woodroffe and Biribo, 2011).

412 On Piddington Mound, the location and distribution of the "Live coral framework" area is
413 interesting as live coral framework is typically found at or near the summit of mounds
414 (Rüggeberg *et al.*, 2011). However, the main loci for live coral growth on different mounds
415 varies from setting to setting: on the summit (e.g. Galway Mound: Dorschel *et al.* (2007), the
416 lee side of the mound structure (e.g. Giant Mound and the Hedge Mounds: Dorschel et al.,
417 2009), and to the current-facing side of the mound structure (e.g. CWC reefs at Hola, offshore
418 Norway: (Buhl-Mortenson *et al.*, 2015). In the case of the Piddington Mound, it occurs just
419 north of the summit (Fig. 6) on the lee side of the mound. In areas of excessively high current
420 flow on the Porcupine Bank, CWC have been found flourishing on the lee-side of mounds
421 (Dorschel *et al.*, 2009). However, this is unlike other mounds in the eastern Porcupine Seabight
422 (i.e. Galway Mound: Dorschel et al., 2007), and here the summit of Piddington Mound is
423 dominated by Coral rubble facies. Fig. 3C maps the facies types across the Piddington Mound
424 bathymetric cross-profile. Lim (2017) measure a current speed here of 39 - 41 cm s^{-1} in this
425 area, the highest noted for the western Moira Mounds chain. It may be that the live corals in
426 F2 thrive in the shelter provided by the mound which acts as a physical barrier slowing the
427 currents. Purser *et al.* (2010) and Orejas *et al.* (2016) show that *Lophelia* capture food more
428 effectively in lower flow velocities. However, whilst these are laboratory-based studies, a

detailed study from the Mingulay Reef Complex may also explain the distribution of live corals on the Piddington Mound where mound topography-induced turbulence may account for enhanced delivery of food particles suspended in deeper water (see Davies *et al.*, 2009).

The facies zonation observed on the Piddington Mound has various implications for the interpretation of coral deposits in fossil outcrop. Coral diversity, coral morphology, sediment-type (hydrodynamic energy), presence of algae, abundance of pelagic or planktonic components, microborings, surrounding facies or geochemistry are among the numerous recognition criteria to distinguish between shallow- or deep-water occurring CWC mound deposits (Mullins *et al.*, 1981). With more studies available on modern CWC mounds, Hebbeln and Samankassou (2015) show that misinterpretation of some of these distinguishing criteria are possible and, in fact, for many ancient carbonate mounds, formation in deep water appear just as likely as formation in shallow shelf seas. In line with this argument, various comparisons have been outlined herein between the Piddington Mound and shallow water reef atolls. In addition, facies zonations appear common in both modern, shallow-water coral reef build ups (Janßen *et al.*, 2017) and in outcrops (Gischler, 1995; Reolid *et al.*, 2014). Here, the first deep-water CWC mound video mosaic also exhibits a reef-scale facies zonation. Thus, these similarities must also be taken into consideration when interpreting fossil coral outcrops.

5. Conclusion

Although video mosaicking an entire CWC reef at this resolution is time consuming in data acquisition, processing and analysis, our preliminary investigation offers new, unique and detailed insights to CWC reef organisation and facies distribution. Despite mound surface heterogeneity, areas of the Piddington Mound surface (as small as 0.25 m^2) cluster significantly in a ring-like pattern focussed around the mound summit. While ring-like observations have

been reported at other CWC mounds (e.g. Henriet *et al.*, 1998; Wilson, 1979), the facies pattern here is physically dissimilar. A definitive explanation cannot be put forward for the existence of this ring-like facies pattern however, a scenario is put forward based on the influences of the surrounding environment drawing parallels to shallow-water coral atolls. The existence of a facies zonation implies that deep-water CWC mounds are similar to shallow-water coral build-ups and this should be taken into consideration when making interpretations from fossil coral outcrops.

Looking to the future, this data set may be used to either compare supervised and unsupervised classification techniques or to ground-truth high-resolution facies distribution prediction models.

6. Acknowledgements

The authors would like to thank Dr. Jürgen Titschack and an anonymous reviewer for their time and effort in extremely useful and constructive reviews. Further, the authors would like to thank the crew and officers of ROV Holland 1 and RV Celtic Explorer for assistance in collecting high resolution, accurately positioned data. Ship time on the RV Celtic Explorer was funded by the Marine Institute under the 2011 and 2015 Ship Time Programme of the National Development Plan. Aaron Lim is funded by the Irish Research Council Graduate of Ireland Scholarship IRC (2015 - 2016).

7. References

Anselin, L., 1995. Local Indicators of Spatial Association—LISA. Geographical Analysis 27 (2), 93-115, 10.1111/j.1538-4632.1995.tb00338.x.

476 Beyer, A., Schenke, H.W., Klenke, M., Niederjasper, F., 2003. High resolution bathymetry of
477 the eastern slope of the Porcupine Seabight. Marine Geology 198 (1-2), 27-54,
478 http://dx.doi.org/10.1016/S0025-3227(03)00093-8.

479 Buhl-Mortenson, L., Hodnesdal, H., Thorsnes, T., 2015. The Norwegian Sea Floor.
480 MAREANO 2015,

481 Burt, P.J., Adelson, E.H., 1983. A Multiresolution Spline with Application to Image Mosaics.
482 Acm Transactions on Graphics 2 (4), 217-236, Doi 10.1145/245.247.

483 Chevalier, J.-P., 1968. Etude géomorphologique et bionomique de l'atoll de Mururoa
484 (Tuamotu),

485 Correa, T.B.S., Eberli, G.P., Grasmueck, M., Reed, J.K., Correa, A.M.S., 2012a. Genesis and
486 morphology of cold-water coral ridges in a unidirectional current regime. Marine Geology
487 326, 14-27, 10.1016/j.margeo.2012.06.008.

488 Correa, T.B.S., Grasmueck, M., Eberli, G.P., Reed, J.K., Verwer, K., Purkis, S.A.M., 2012b.
489 Variability of cold-water coral mounds in a high sediment input and tidal current regime,
490 Straits of Florida. Sedimentology 59 (4), 1278-1304, 10.1111/j.1365-3091.2011.01306.x.

491 Coughlan, M., Wheeler, A.J., Dorschel, B., Lordan, C., Boer, W., Gaever, P.v., Haas, H.d.,
492 Mörz, T., 2015. Record of anthropogenic impact on the Western Irish Sea mud belt.
493 Anthropocene 9, 56-69, http://dx.doi.org/10.1016/j.ancene.2015.06.001.

494 Davies, A.J., Duineveld, G.C., Lavaleye, M.S., Bergman, M.J., van Haren, H., Roberts, J.M.,
495 2009. Downwelling and deep-water bottom currents as food supply mechanisms to the cold-
496 water coral Lophelia pertusa (Scleractinia) at the Mingulay Reef complex. Limnology and
497 Oceanography 54 (2), 620, DOI 10.4319/lo.2009.54.2.0620.

498 Davies, A.J., Wisshak, M., Orr, J.C., Murray Roberts, J., 2008. Predicting suitable habitat for
499 the cold-water coral Lophelia pertusa (Scleractinia). Deep Sea Research Part I:
500 Oceanographic Research Papers 55 (8), 1048-1062, 10.1016/j.dsr.2008.04.010.

501 De Mol, B., Kozachenko, M., Wheeler, A.J., Alvares, H., Henriet, J.-P., Olu-Le Roy, K.,
502 2007. Thérèse Mound: a case study of coral bank development in the Belgica Mound
503 Province, Porcupine Seabight. International Journal of Earth Sciences 96 (1), 103-120,
504 http://dx.doi.org/10.1007/s00531-005-0496-x.

505 Dolan, M.F.J., Grehan, A.J., Guinan, J.C., Brown, C., 2008. Modelling the local distribution
506 of cold-water corals in relation to bathymetric variables: Adding spatial context to deep-sea
507 video data. Deep-Sea Research I 55 (11), 1564-1579,
508 http://dx.doi.org/10.1016/j.dsr.2008.06.010.

509 Dorschel, B., Hebbeln, D., Foubert, A., White, M., Wheeler, A.J., 2007. Hydrodynamics and
510 cold-water coral facies distribution related to recent sedimentary processes at Galway Mound
511 west of Ireland. Marine Geology 244 (1–4), 184-195,
512 http://dx.doi.org/10.1016/j.margeo.2007.06.010.

513 Dorschel, B., Wheeler, A.J., Huvenne, V.A.I., de Haas, H., 2009. Cold-water coral mounds in
514 an erosive environmental setting: TOBI side-scan sonar data and ROV video footage from

515 the northwest Porcupine Bank, NE Atlantic. Marine Geology 264 (3-4), 218-229,
516 10.1016/j.margeo.2009.06.005.

517 Dorschel, B., Wheeler, A.J., Monteys, X., Verbruggen, K., 2010. Atlas of the Deep-water
518 Seabed: Ireland. Springer, Dordrecht Heidelberg London New York DOI 10.1007/978-90-
519 481-9376-1.

520 Douarin, M., Sinclair, D.J., Elliot, M., Henry, L.-A., Long, D., Mitchison, F., Roberts, J.M.,
521 2014. Changes in fossil assemblage in sediment cores from Mingulay Reef Complex (NE
522 Atlantic): Implications for coral reef build-up. Deep Sea Research Part II: Topical Studies in
523 Oceanography 99, 286-296, http://dx.doi.org/10.1016/j.dsr2.2013.07.022.

524 Dullo, C., Flögel, S., Rüggeberg, A., 2008. Cold-water coral growth in relation to the
525 hydrography of the Celtic and Nordic European continental margin. Marine Ecology Progress
526 Series 371, 165-176, 10.3354/meps07623.

527 Eisele, M., Hebbeln, D., Wienberg, C., 2008. Growth history of a cold-water coral covered
528 carbonate mound - Galway Mound, Porcupine Seabight, NE-Atlantic. Marine Geology 253
529 (3-4), 160-169, 10.1016/j.margeo.2008.05.006.

530 Ferrer, J., Elibol, A., Delaunoy, O., Gracias, N., Garcia, R., 2007. Large-area photo-mosaics
531 using global alignment and navigation data. MTS/IEEE OCEANS Conference, Vancouver,
532 Canada, pp. 1-9^, http://dx.doi.org/10.1109/OCEANS.2007.4449367.

533 Foubert, A.T.G., Beck, T., Wheeler, A.J., Opderbecke, J., Grehan, A., Klages, M., Thiede, J.,
534 Henriet, J.-P., Polarstern ARK-XIX/3a shipboard party, 2005. New view of the Belgica
535 Mounds, Porcupine Seabight, NE Atlantic: preliminary results from the Polarstern ARK-
536 XIX/3a ROV cruise. In: Freiwald, A., Roberts, J.M. (Eds.), Deep-water corals and
537 Ecosystems, . Springer-Verlag, Berlin Heidelberg, pp. 403-415,

538 Foubert, A.T.G., Depreiter, D., Beck, T., Maignien, L., Pannemans, B., Frank, N., Blamart,
539 D., Henriet, J.-P., 2008. Carbonate mounds in a mud volcano province off north-west
540 Morocco: Key to processes and controls. Marine Geology 248, 74-96,

541 Foubert, A.T.G., Huvenne, V.A.I., Wheeler, A.J., Kozachenko, M., Opderbecke, J., Henriet,
542 J.-P., 2011. The Moira Mounds, small cold-water coral mounds in the Porcupine Seabight,
543 NE Atlantic: Part B - Evaluating the impact of sediment dynamics through high-resolution
544 ROV-borne bathymetric mapping Marine Geology 282 (1-2), 65-78,
545 doi:10.1016/j.margeo.2011.02.008

546 Freiwald, A., 2002. Reef-Forming Cold-Water Corals. In: Wefer, G., Billett, D.S.M.,
547 Hebbeln, D., Jørgensen, B.B., van Weering, T.C.E. (Eds.), Ocean Margin Systems. Springer,
548 Berlin Heidelberg New York, pp. 365-385, http://dx.doi.org/10.1007/978-3-662-05127-6_23.

549 Freiwald, A., Fosså, J.H., Grehan, A., Koslow, T., Roberts, J.M., 2004. Cold-water coral
550 reefs. UNEP-WCMC, Cambridge, UK 84,

551 Getis, A., Ord, J.K., 1992. The Analysis of Spatial Association by Use of Distance Statistics.
552 Geographical Analysis 24 (3), 189-206, 10.1111/j.1538-4632.1992.tb00261.x.

553 Gischler, E., 1995. Current and Wind Induced Facies Patterns in a Devonian Atoll: Iberg
554 Reef, Harz Mts., Germany. Palaios 10 (2), 180-189, 10.2307/3515181.

555 Goodchild, M., 1986. Spatial Autocorrelation. Concepts and Techniques in Modern
556 Geography 47. Norwich, UK: Geo Books,
557 https://alexsingleton.files.wordpress.com/2014/09/47-spatial-aurocorrelation.pdf

558 Guinan, J., Grehan, A.J., Dolan, M.F.J., Brown, C., 2009. Quantifying relationships between
559 video observations of cold-water coral cover and seafloor features in Rockall Trough, west of
560 Ireland. Marine Ecology Progress Series 375, 125-138, 10.3354/meps07739.

561 Hebbeln, D., Samankassou, E., 2015. Where did ancient carbonate mounds grow — In
562 bathyal depths or in shallow shelf waters? Earth-Science Reviews 145, 56-65,
563 http://dx.doi.org/10.1016/j.earscirev.2015.03.001.

564 Hebbeln, D., Wienberg, C., Wintersteller, P., Freiwald, A., Becker, M., Beuck, L., Dullo, C.,
565 Eberli, G.P., Glogowski, S., Matos, L., 2014. Environmental forcing of the Campeche cold-
566 water coral province, southern Gulf of Mexico.

567 Heindel, K., Titschack, J., Dorschel, B., Huvenne, V.A.I., Freiwald, A., 2010. The sediment
568 composition and predictive mapping of facies on the Propeller Mound—A cold-water coral
569 mound (Porcupine Seabight, NE Atlantic). Continental Shelf Research 30 (17), 1814-1829,
570 doi:10.1016/j.csr.2010.08.007.

571 Henriet, J.-P., De Mol, B., Pillen, S., Vanneste, M., Van Rooij, D., Versteeg, W., Croker,
572 P.F., Shannon, P.M., Unnithan, V., Bouriak, S., Chachkine, P., BELGICA 97 Shipboard
573 scientific crew, 1998. Gas hydrate crystals may help build reefs. Nature 391 (6668), 648-649,
574 Doi 10.1038/35530.

575 Huang, Z., Brooke, B.P., Harris, P.T., 2011. A new approach to mapping marine benthic
576 habitats using physical environmental data. Continental Shelf Research 31 (2, Supplement),
577 S4-S16, http://dx.doi.org/10.1016/j.csr.2010.03.012.

578 Huvenne, V.A., Tyler, P.A., Masson, D.G., Fisher, E.H., Hauton, C., Huhnerbach, V., Le
579 Bas, T.P., Wolff, G.A., 2011. A picture on the wall: innovative mapping reveals cold-water
580 coral refuge in submarine canyon. PLoS ONE 6 (12), e28755, 10.1371/journal.pone.0028755.

581 Huvenne, V.A.I., Bett, B.J., Masson, D.G., Le Bas, T.P., Wheeler, A.J., 2016. Effectiveness
582 of a deep-sea cold-water coral Marine Protected Area, following eight years of fisheries
583 closure. Biological Conservation 200, 60-69, 10.1016/j.biocon.2016.05.030.

584 Huvenne, V.A.I., Beyer, A., de Haas, H., Dekindt, K., Henriet, J.-P., Kozachenko, M., Olu-
585 Le Roy, K., Wheeler, A.J., participants, T.P.c., participants, C.c., 2005. The seabed
586 appearance of different coral bank provinces in the Porcupine Seabight, NE Atlantic: results
587 from sidescan sonar and ROV seabed mapping. In: Freiwald, A., Roberts, J.M. (Eds.), Cold-
588 water Corals and Ecosystems. Springer-Verlag, Berlin Heidelberg, pp. 535-569,
589 http://dx.doi.org/10.1007/3-540-27673-4_27.

590 Huvenne, V.A.I., Blondel, P., Henriet, J.-P., 2002. Textural analyses of sidescan sonar
591 imagery from two mound provinces in the Porcupine Seabight. Marine Geology 189 (3-4),
592 323-341, Pii Doi 10.1016/S0025-3227(02)00420-6.

593 Huvenne, V.A.I., Van Rooij, D., De Mol, B., Thierens, M., O'Donnell, R., Foubert, A.T.G.,
594 2009. Sediment dynamics and palaeo-environmental context at key stages in the Challenger

595 cold-water coral mound formation: Clues from sediment deposits at the mound base. Deep
596 Sea Research Part I 56 (12), 2263-2280, 10.1016/j.dsr.2009.08.003.

597 IODP 307 Expedition scientists, 2005. Modern carbonate mounds: Porcupine drilling. IODP
598 Prel. Rept., 307. p. 58, doi:10.2204/iodp.pr.307.2005

599 Janßen, A., Wizemann, A., Klicpera, A., Satari, D.Y., Westphal, H., Mann, T., 2017.
600 Sediment Composition and Facies of Coral Reef Islands in the Spermonde Archipelago,
601 Indonesia. Frontiers in Marine Science 4 (144), 10.3389/fmars.2017.00144.

602 Kano, A., Ferdelman, T.G., Williams, T., Henriet, J.-P., Ishikawa, T., Kawagoe, N.,
603 Takashima, C., Kakizaki, Y., Abe, K., Sakai, S., Browning, E.L., Li, X., Andres, M.S.,
604 Bjerager, M., Cragg, B.A., De Mol, B., Dorschel, B., Foubert, A.T.G., Frank, T.D., Fuwa, Y.,
605 Gaillot, P., Gharib, J.J., Gregg, J.M., Huvenne, V.A.I., Léonide, P., Mangelsdorf, K.,
606 Monteys, X., Novosel, I., O'Donnell, R., Rüggeberg, A., Samarkin, V.A., Sasaki, K.,
607 Spivack, A.J., Tanaka, A., Titschack, J., van Rooij, D., Wheeler, A.J., 2007. Age constraints
608 on the origin and growth history of a deep-water coral mound in the northeast Atlantic drilled
609 during Integrated Ocean Drilling Program Expedition 307. Geology 35 (11), 1051-1054, doi:
610 10.1130/G23917A.

611 Kocak, D.M., Caimi, F.M., 2005. The Current Art of Underwater Imaging – With a
612 Glimpse of the Past and Vision of the Future. Marine Technology Society Journal 39 (3), 5-
613 26, 10.4031/002533205787442576.

614 Kozachenko, M., 2005. Present and Past Environments of the Belgica Mounds (deep-water
615 coral carbonate mounds) Eastern Porcupine Seabight, North East Atlantic (unpublished PhD
616 Thesis), University College Cork, Cork,

617 Kwatra, V., Schödl, A., Essa, I., Turk, G., Bobick, A., 2003. Graphcut textures: image and
618 video synthesis using graph cuts. ACM Transactions on Graphics (TOG). ACM, pp. 277-
619 286^, http://dx.doi.org/10.1145/882262.882264.

620 Lamarche, G., Lurton, X., Verdier, A.-L., Augustin, J.-M., 2011. Quantitative
621 characterisation of seafloor substrate and bedforms using advanced processing of multibeam
622 backscatter—Application to Cook Strait, New Zealand. Continental Shelf Research 31 (2,
623 Supplement), S93-S109, http://dx.doi.org/10.1016/j.csr.2010.06.001.

624 Lim, A., 2017. Spatio-temporal patterns and controls on cold-water coral reef development:
625 the Moira Mounds, Porcupine Seabight, NE Atlantic, University College Cork, Cork Open
626 Research Archive, http://hdl.handle.net/10468/4031.

627 Lirman, D., Gracias, N.R., Gintert, B.E., Gleason, A.C.R., Reid, R.P., Negahdaripour, S.,
628 Kramer, P., 2007. Development and application of a video-mosaic survey technology to
629 document the status of coral reef communities. Environmental Monitoring and Assessment
630 125 (1), 59-73, 10.1007/s10661-006-9239-0.

631 Lowe, D.G., 1999. Object recognition from local scale-invariant features. Computer vision,
632 1999. The proceedings of the seventh IEEE international conference on Computer Vision.
633 Ieee, pp. 1150-1157^, http://dx.doi.org/10.1109/ICCV.1999.790410.

634 Messing, C.G., Neumann, A.C., Lang, J.C., 1990. Biozonation of deep-water lithoherms and
635 associated hardgrounds in the northeastern Straits of Florida. Palaios 5, 15-33,

636 Mienis, F., de Stigter, H.C., de Haas, H., van Weering, T.C.E., 2009. Near-bed particle
637 deposition and resuspension in a cold-water coral mound area at the Southwest Rockall
638 Trough margin, NE Atlantic. Deep Sea Research Part I: Oceanographic Research Papers 56
639 (6), 1026-1038, http://dx.doi.org/10.1016/j.dsr.2009.01.006.

640 Mullins, H.T., Newton, C.R., Heath, K., Van Buren, H.M., 1981. Modern deep-water coral
641 mounds north of Little Bahama Bank; criteria for recognition of deep-water coral bioherms in
642 the rock record. Journal of sedimentary research 51 (3), 999-1013, 10.1306/212f7dfb-2b24-
643 11d7-8648000102c1865d.

644 Murphy, P., Wheeler, A.J., 2017. A GIS-based application of drainage basin analysis and
645 geomorphometry in the submarine environment: The Gollum Canyon System, North-east
646 Atlantic. In: Bartlett, D., Celliers, L. (Eds.), Geoinformatics for Marine and Coastal
647 Management. CRC Press, Taylor & Francis Group, Boca Raton, USA,
648 http://dx.doi.org/10.1201/9781315181523-4.

649 Ord, J.K., Getis, A., 1995. Local Spatial Autocorrelation Statistics: Distributional Issues and
650 an Application. Geographical Analysis 27 (4), 286-306, 10.1111/j.1538-
651 4632.1995.tb00912.x.

652 Orejas, C., Gori, A., Rad-Menendez, C., Last, K.S., Davies, A.J., Beveridge, C.M., Sadd, D.,
653 Kiriakoulakis, K., Witte, U., Roberts, J.M., 2016. The effect of flow speed and food size on
654 the capture efficiency and feeding behaviour of the cold-water coral Lophelia pertusa. Journal
655 of Experimental Marine Biology and Ecology 481, 34-40, 10.1016/j.jembe.2016.04.002.

656 Purser, A., 2015. A Time Series Study of Lophelia pertusa and Reef Megafauna Responses to
657 Drill Cuttings Exposure on the Norwegian Margin. PLoS ONE 10 (7), e0134076,
658 10.1371/journal.pone.0134076.

659 Purser, A., Larsson, A.I., Thomsen, L., van Oevelen, D., 2010. The influence of flow velocity
660 and food concentration on *Lophelia pertusa* (Scleractinia) zooplankton capture rates. Journal
661 of Experimental Marine Biology and Ecology 395 (1-2), 55-62,
662 10.1016/j.jembe.2010.08.013.

663 Reolid, J., Betzler, C., Braga, J.C., Martín, J.M., Lindhorst, S., Reijmer, J.J.G., 2014. Reef
664 slope geometries and facies distribution: controlling factors (Messinian, SE Spain). Facies 60
665 (3), 737-753, 10.1007/s10347-014-0406-4.

666 Roberts, J.M., Brown, C.J., Long, D., Bates, C.R., 2005. Acoustic mapping using a
667 multibeam echosounder reveals cold-water coral reefs and surrounding habitats. Coral Reefs
668 24 (4), 654-669, 10.1007/s00338-005-0049-6.

669 Roberts, J.M., Long, D., Wilson, J.B., Mortensen, P.B., Gage, J.D., 2003. The cold-water
670 coral Lophelia pertusa (Scleractinia) and enigmatic seabed mounds along the north-east
671 Atlantic margin: are they related? Marine Pollution Bulletin 46 (1), 7-20,
672 http://dx.doi.org/10.1016/S0025-326X(02)00259-X.

673 Roberts, J.M., Wheeler, A., Freiwald, A., Cairns, S., 2009. Cold-Water Corals: The Biology
674 and Geology of Deep-Sea Coral Habitats. Cambridge University Press,
675 http://books.google.ie/books?id=6WA3YIH27t0C

676 Roberts, J.M., Wheeler, A.J., Freiwald, A., 2006. Reefs of the Deep: The Biology and
677 Geology of Cold-Water Coral Ecosystems. Science 312 (5773), 543-547,
678 http://dx.doi.org/10.1126/science.1119861.

679 Rüggeberg, A., Flögel, S., Dullo, W.-C., Hissmann, K., Freiwald, A., 2011. Water mass
680 characteristics and sill dynamics in a subpolar cold-water coral reef setting at Stjernsund,
681 northern Norway. Marine Geology 282 (1–2), 5-12,
682 http://dx.doi.org/10.1016/j.margeo.2010.05.009.

683 Rzhanov, Y., Linnett, L.M., Forbes, R., 2000. Underwater video mosaicing for seabed
684 mapping. Image Processing, 2000. Proceedings. 2000 International Conference on, pp. 224-
685 227 vol.221^, 10.1109/ICIP.2000.900935.

686 Savini, A., Vertino, A., Marchese, F., Beuck, L., Freiwald, A., 2014. Mapping cold-water
687 coral habitats at different scales within the Northern Ionian Sea (Central Mediterranean): an
688 assessment of coral coverage and associated vulnerability. PLoS ONE 9 (1), e87108,
689 10.1371/journal.pone.0087108.

690 Spezzaferri, S., Vertino, A., Addamo, A.M., Backers, J., Baratti, V., Constandache, M.,
691 Camozzi, O., El Kateb, A., Gennari, G., Leuzinger, L., McGrath, M., Mc Hugh, S.K., Naudts,
692 L., Savini, A., Stalder, C., 2012. E-CWC Moira (2012/16) *RV Belgica*: Cold-water coral
693 ecosystems from the Moira Mounds (NE Atlantic): affinities and differences with modern
694 and Pleistocene Mediterranean counterparts. University Freibourg, Switzerland, Unpublished
695 Cruise Report,

696 Squires, D.F., 1964. Fossil coral thickets in Wairarapa, New Zealand. Journal Paleontol. 38
697 (5), 904-915, http://www.jstor.org/stable/1301611

698 Thierens, M., Titschack, J., Dorschel, B., Huvenne, V.A.I., Wheeler, A.J., Stuut, J.-B.W.,
699 O'Donnell, R., 2010. The 2.6 Ma depositional sequence from the Challenger cold-water coral
700 carbonate mound (IODP Exp. 307): sediment contributors and hydrodynamic palaeo-
701 environments. Marine Geology 271 (3-4), 260-277, doi:10.1016/j.margeo.2010.02.021.

702 Titschack, J., Thierens, M., Dorschel, B., Schulbert, C., Freiwald, A., Kano, A., Takashima,
703 C., Kawagoe, N., Li, X., 2009. Carbonate budget of a cold-water coral mound (Challenger
704 Mound, IODP Exp. 307). Marine Geology 259 (1-4), 36-46, 10.1016/j.margeo.2008.12.007.

705 Van Rooij, D., 2004. An integrated study of Quaternary sedimentary processes on the eastern
706 slope of the Porcupine Seabight, SW of Ireland, Ghent University,
707 http://dx.doi.org/1854/10815.

708 Vertino, A., Savini, A., Rosso, A., Di Geronimo, I., Mastrototaro, F., Sanfilippo, R., Gay, G.,
709 Etiope, G., 2010. Benthic habitat characterization and distribution from two representative
710 sites of the deep-water SML Coral Province (Mediterranean). Deep-Sea Research Part Ii-
711 Topical Studies in Oceanography 57 (5-6), 380-396, 10.1016/j.dsr2.2009.08.023.

712 Vertino, A., Spezzaferri, S., Ruggeberg, A., Stalder, C., Wheeler, A.J., Party, t.E.C.-M.c.S.,
713 2015. An Overview on Cold-Water Coral Ecosystems and Facies. In: Spezzaferri, S.,
714 Ruggeberg, A., Stalder, C. (Eds.), Atlas of benthic foraminifera from cold-water coral reefs.
715 Cushman Foundation for Foraminiferal Research, pp. 12-19,

716 Wheeler, A.J., Beyer, A., Freiwald, A., de Haas, H., Huvenne, V.A.I., Kozachenko, M., Olu-
717 Le Roy, K., Opderbecke, J., 2007. Morphology and environment of cold-water coral
718 carbonate mounds on the NW European margin. International Journal of Earth Sciences 96
719 (1), 37-56, http://dx.doi.org/10.1007/s00531-006-0130-6.

720 Wheeler, A.J., Capocci, R., Crippa, L., Connolly, N., Hogan, R., Lim, A., McCarthy, E.,
721 McGonigle, C., O' Donnell, E., O' Sullivan, K., Power, K., Ryan, G., Vertino, A., Holland 1
722 ROV Technical Team, Officers and Crew of the RV Celtic Explorer, 2015. Cruise Report:
723 Quantifying Environmental Controls on Cold-Water coral Reef Growth (QuERCi).
724 University College Cork, Ireland,

725 Wheeler, A.J., Kozachenko, M., Beyer, A., Foubert, A.T.G., Huvenne, V.A.I., Klages, M.,
726 Masson, D.G., Olu-Le Roy, K., Thiede, J., 2005. Sedimentary processes and carbonate
727 mounds in the Belgica Mound province, Porcupine Seabight, NE Atlantic. In: Freiwald, A.,
728 Roberts, J.M. (Eds.), Cold-water Corals and Ecosystems. Springer-Verlag, Berlin Heidelberg,
729 pp. 533-564, http://dx.doi.org/10.1007/3-540-27673-4_28.

730 Wheeler, A.J., Kozachenko, M., Henry, L.A., Foubert, A., de Haas, H., Huvenne, V.A.I.,
731 Masson, D.G., Olu, K., 2011. The Moira Mounds, small cold-water coral banks in the
732 Porcupine Seabight, NE Atlantic: Part A—an early stage growth phase for future coral
733 carbonate mounds? Marine Geology 282 (1-2), 53-64, 10.1016/j.margeo.2010.08.006.

734 Wheeler, A.J., Kozachenko, M., Masson, D.G., Huvenne, V.A.I., 2008. Influence of benthic
735 sediment transport on cold-water coral bank morphology and growth: the example of the
736 Darwin Mounds, north-east Atlantic. Sedimentology 55 (6), 1875-1887, 10.1111/j.1365-
737 3091.2008.00970.x.

738 Wheeler, A.J., shipboard party, 2011. Vents & Reefs deep-sea ecosystem study of the 45˚
739 North MAR hydrothermal vent field and the cold-water coral Moira Mounds, Porcupine
740 Seabight. Cruise report, p. 160,

741 White, M., Dorschel, B., 2010. The importance of the permanent thermocline to the cold
742 water coral carbonate mound distribution in the NE Atlantic. Earth and Planetary Science
743 Letters 296, 395-402,

744 Wienberg, C., Beuck, L., Heidkamp, S., Hebbeln, D., Freiwald, A., Pfannkuche, O., Monteys,
745 F.X., 2008. Franken Mound: facies and biocoenoses on a newly-discovered “carbonate
746 mound” on the western Rockall Bank, NE Atlantic. Facies 54 (1), 1-24, 10.1007/s10347-007-
747 0118-0.

748 Wienberg, C., Hebbeln, D., Fink, H.G., Mienis, F., Dorschel, B., Vertino, A., López Correa,
749 M., Freiwald, A., 2009. Scleractinian cold-water corals in the Gulf of Cádiz-first clues about
750 their spatial and temporal distribution. Deep Sea Research Part I 56 (10), 1873-1893,
751 doi:10.1016/j.dsr.2009.05.016.

752 Wienberg, C., Wintersteller, P., Beuck, L., Hebbeln, D., 2013. Coral Patch seamount (NE
753 Atlantic) – a sedimentological and megafaunal reconnaissance based on video and
754 hydroacoustic surveys. Biogeosciences 10, 3421-3443, 10.5194/bg-10-3421-2013.

Wilson, J.B., 1979. "Patch" development of the deep-water coral *Lophelia pertusa* (L.) on the Rockall bank. Journal of the Marine Biological Association of the United Kingdom 59 (1), 165-177, http://dx.doi.org/10.1017/S0025315400046257.

Woodroffe, C.D., Biribo, N., 2011. Atolls. In: Hopley, D. (Ed.), Encyclopedia of Modern Coral Reefs: Structure, Form and Process. Springer Netherlands, Dordrecht, pp. 51-71, 10.1007/978-90-481-2639-2_4.

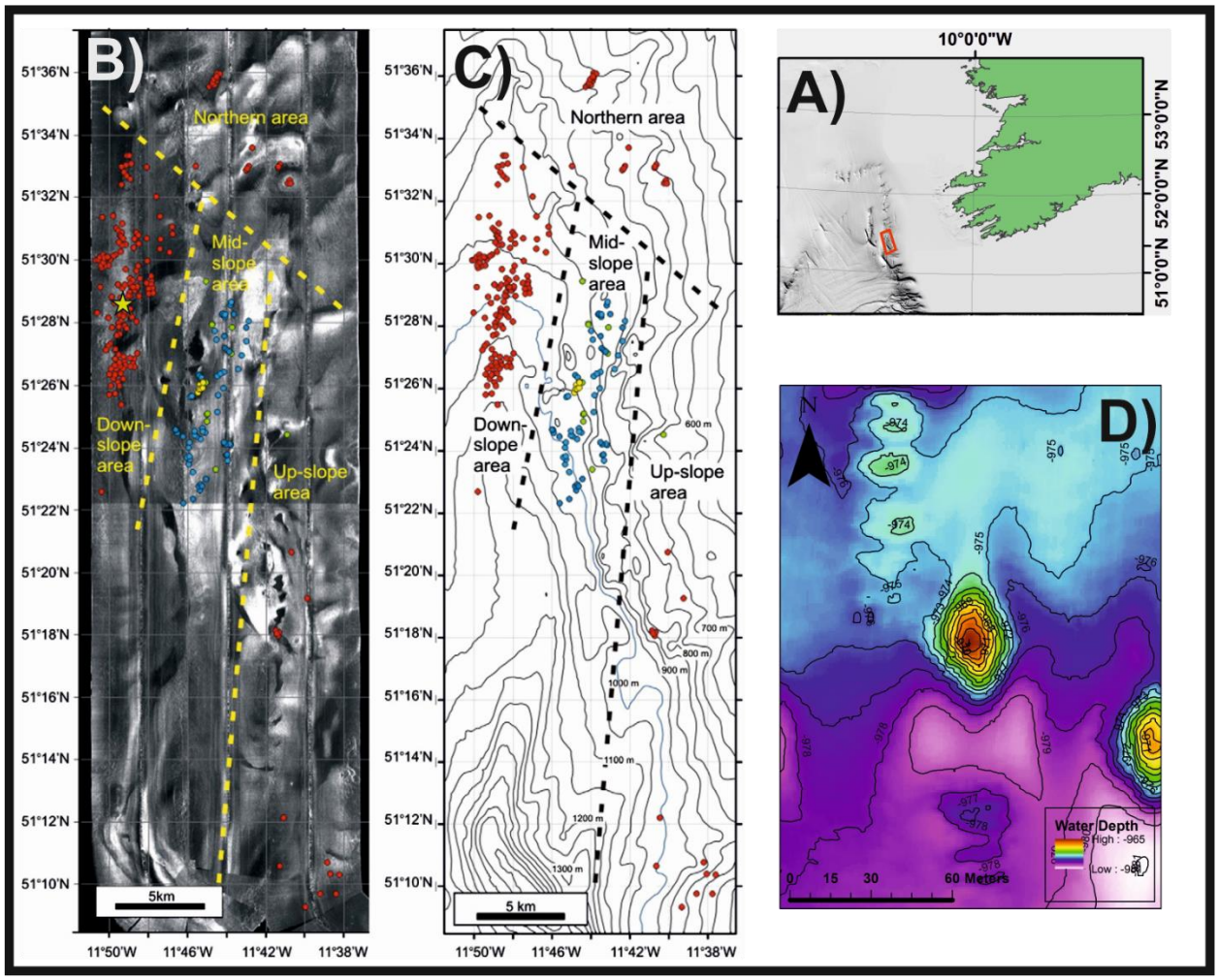

Figure 1 A) Map showing the Belgica Mound Province (BMP) Special Area of Conservation (SAC) (red box) within the Porcupine Seabight relative to Ireland; B) the subdivision of Moira Mounds with the position of the Piddington Mound (yellow star) with side scan sonar data in the background (white tones are high backscatter, darker tones are low backscatter), Red dots= Moira Mounds identified on 30 kHz side-scan sonar data; blue dots=Moira Mounds identified on 100 kHz side-scan sonar data, green dots= Moira Mounds identified on 410 kHz side-scan sonar data; yellow dots= Moira Mounds groundtruthed by ROV and identified on

100 and 410 kHz side-scan sonar after Wheeler et al. (2011); C) the subdivision of Moira Mounds after Wheeler et al. (2011); D) bathymetry of the Piddington Mound area.

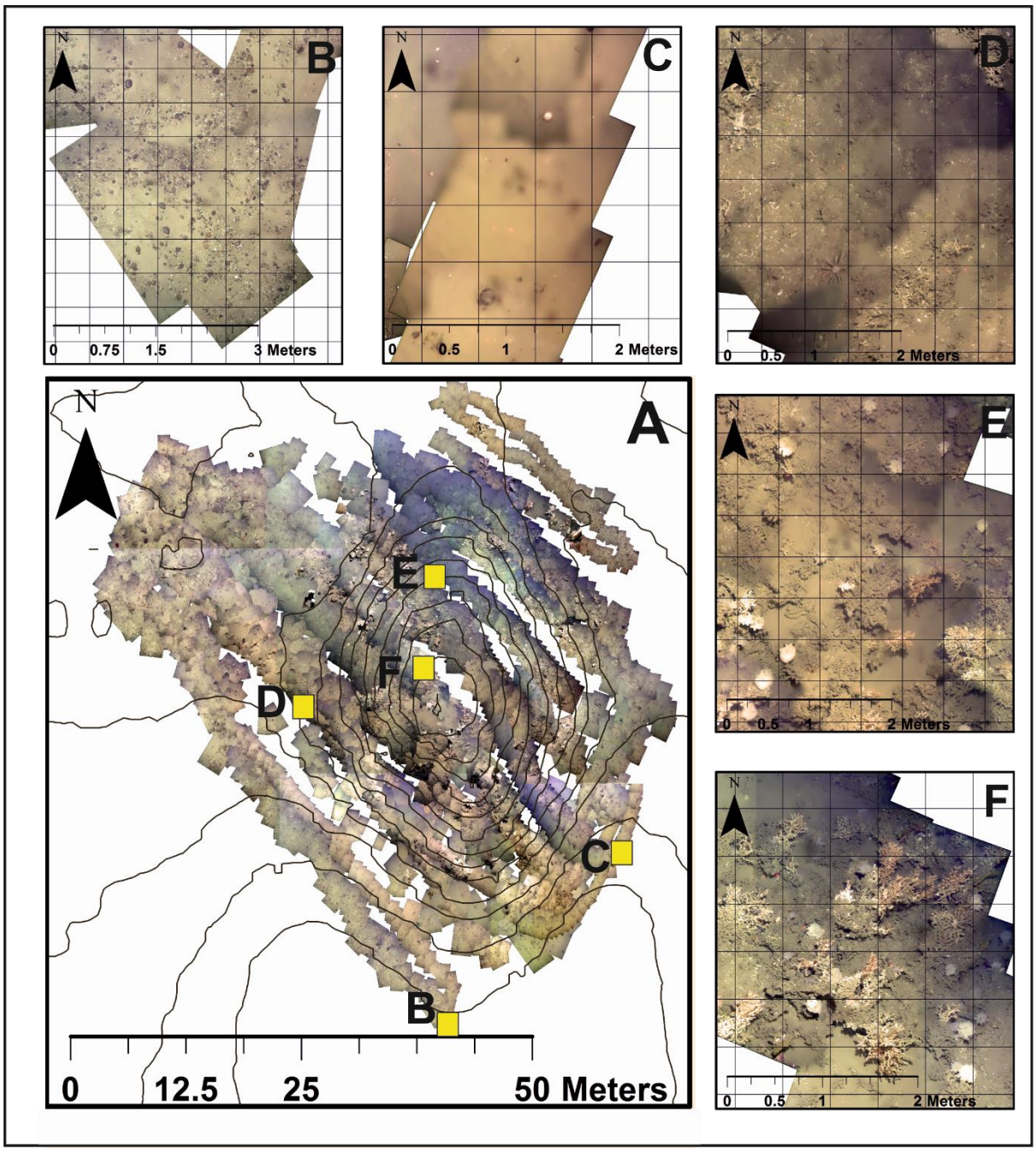

Figure 2 A) Map of georeferenced video mosaic with relative position of close-up images (yellow boxes) with 1 m contours superimposed; B) example close-up image of area dominated by "hemipelagic sediment and dropstone" cells with ArcGIS fishnet overlaid; C) example close-up image of area dominated by "hemipelagic sediment" cells with ArcGIS

776 fishnet overlaid; D) example close-up image of area dominated by “coral rubble” cells with
777 ArcGIS fishnet overlaid; E) example close-up image of area dominated by “dead coral
778 framework” cell with ArcGIS fishnet overlaid; F) example close-up image of area dominated
779 by “live coral framework” cells with ArcGIS fishnet overlaid.

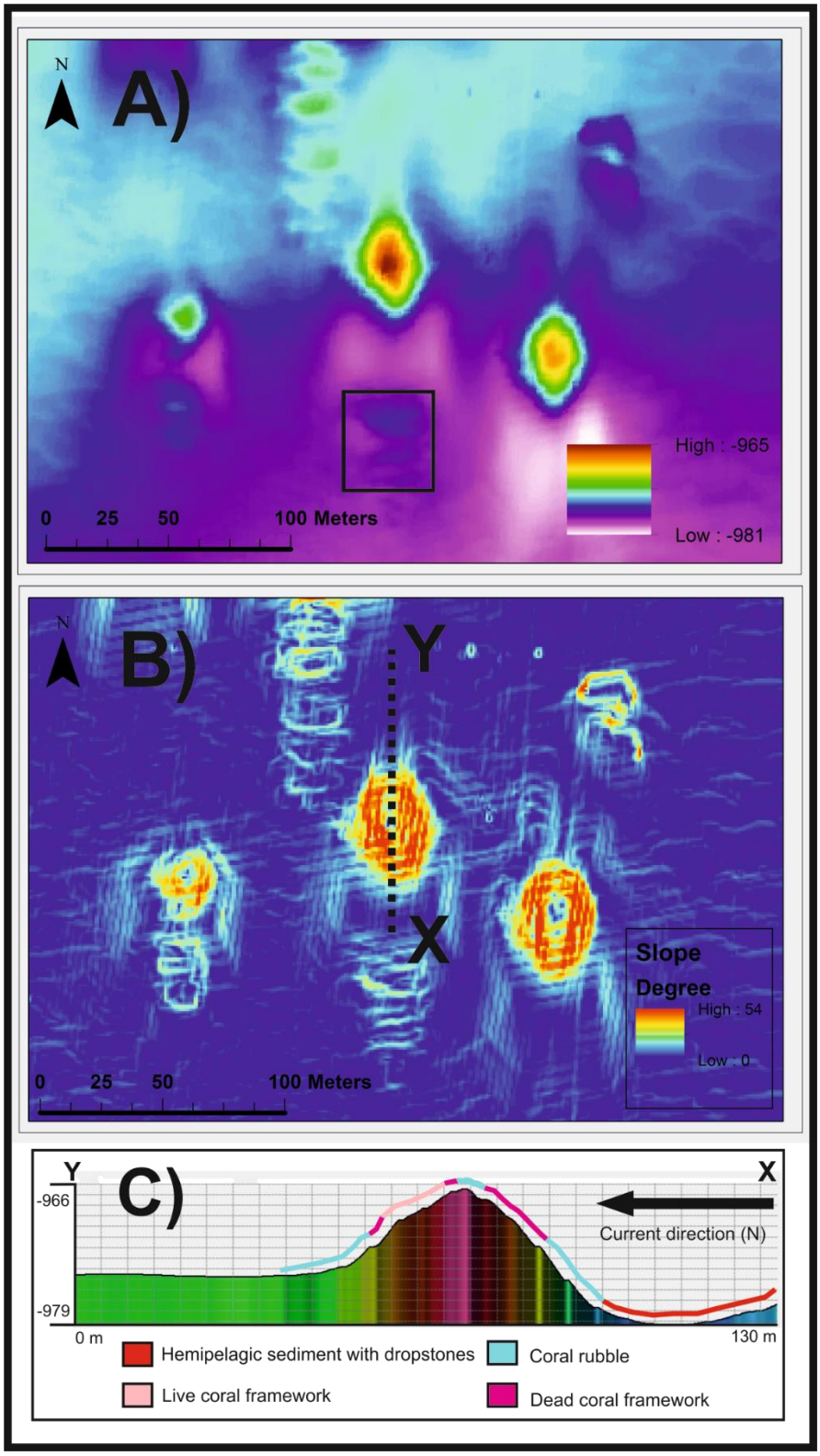

780

781 Figure 3 A) Bathymetry of the Piddington Mound (centre) area with coral ridge feature position

782 identified (black box); B) ArcGIS-generated slope of the Piddington Mound area. Relatively

783 flat areas in blue, relatively steep areas in red and line X-Y (Fig. 3C) indicated; C) Cross profile
784 of Piddington Mound with facies type plotted across the surface.

785

786

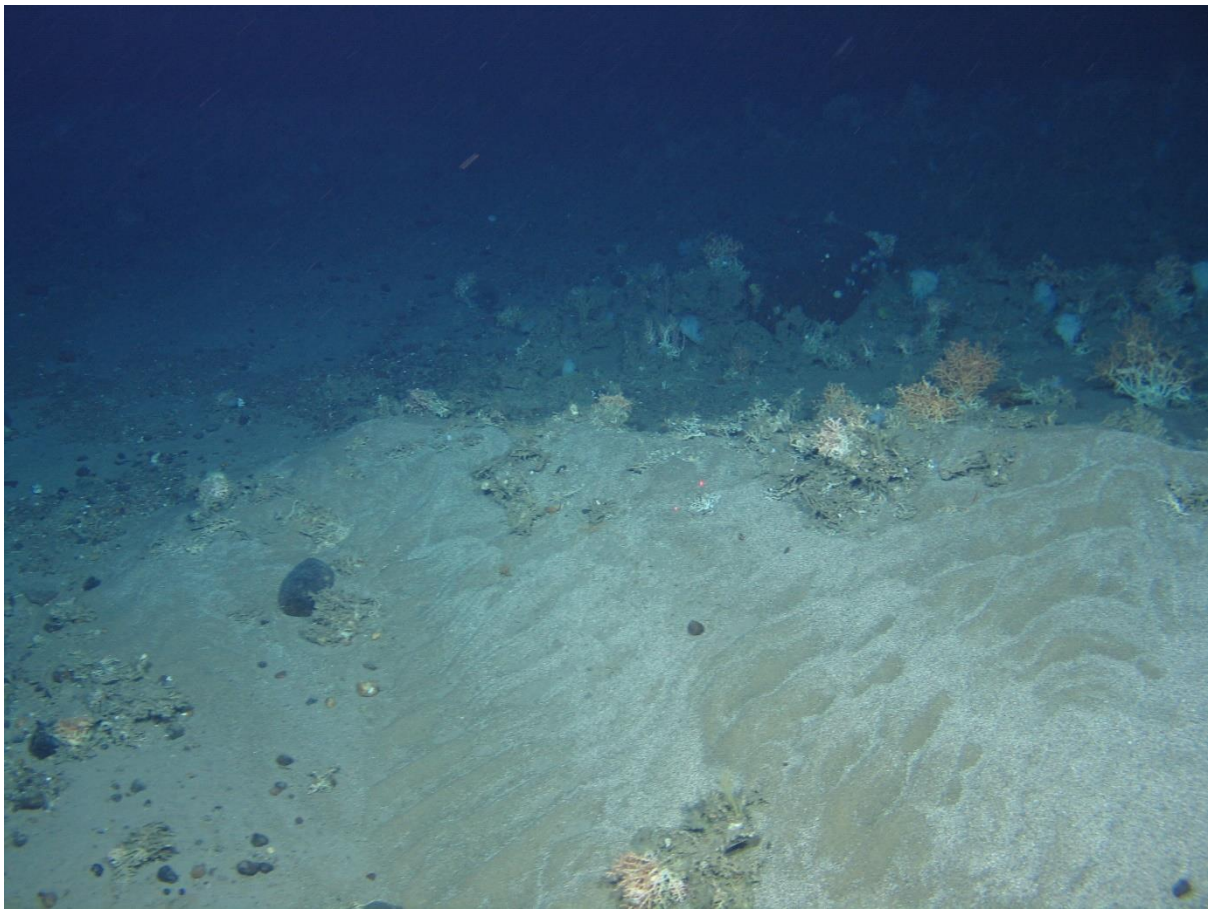

787

788 Figure 4 Image of ridge-form feature, covered with corals to the south of Piddington Mound.
789 View to the north. Laser scalers = 11 cm. Ripple marks on the camera-facing side of the ridge
790 indicate a northerly-directed current.

791

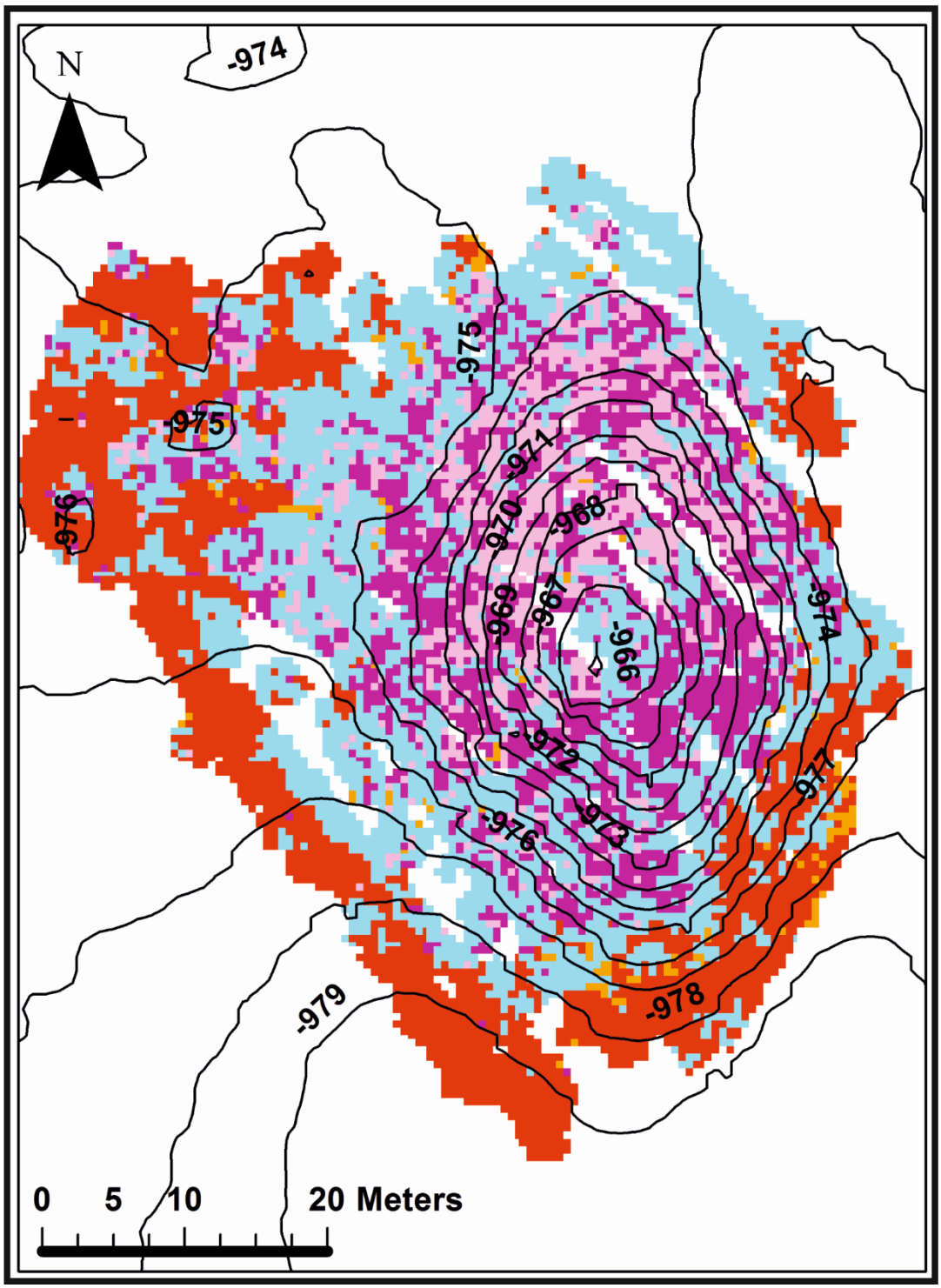

792

793 Figure 5 Classified fishnet *.shp file with contours superimposed showing the distribution of
794 facies types across the Piddington Mound mosaic (red = hemipelagic sediment with dropstones,
795 orange = hemipelagic sediment, blue = coral rubble, purple = dead coral framework, and pink
796 = live coral framework).

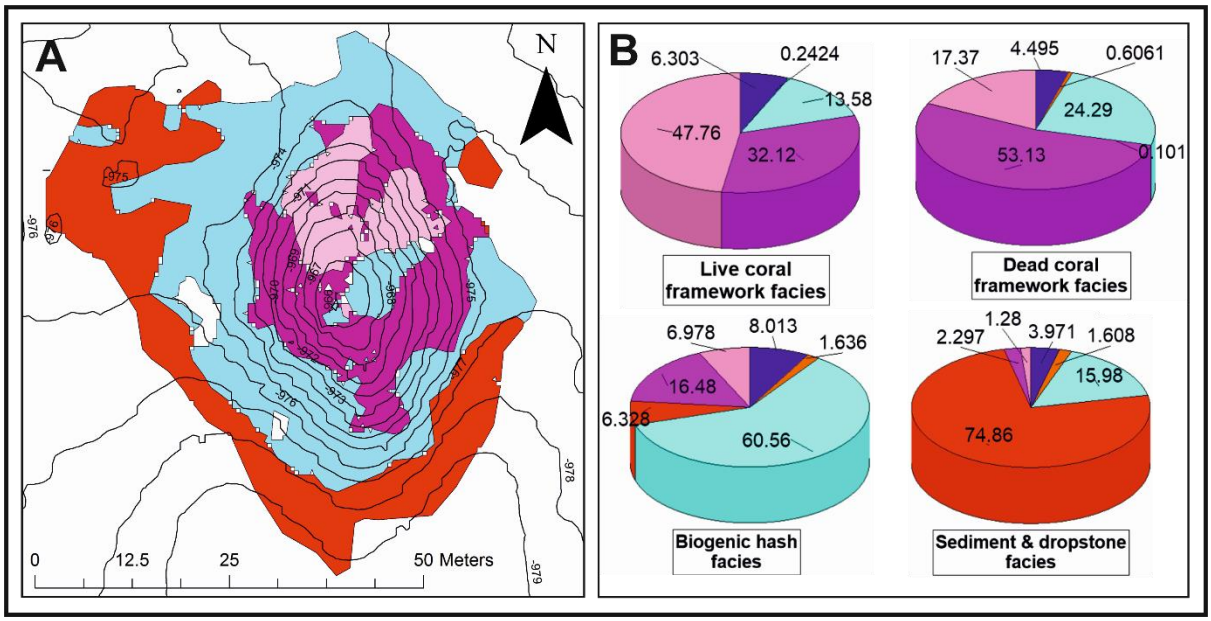

Figure 6 A) Map showing the focal statistics layer which shows the 4 identified facies occurring in 5 areas. Each facies represents where a cell-type is most dominant within a 2.5 m radius neighbourhood (red = “Hemipelagic sediment with dropstones” facies, blue = “Coral rubble” facies, dark pink = “Dead coral framework” facies, light pink = “Live coral framework” facies); B) Pie charts showing the relative proportion and percentages of cells that define each facies.

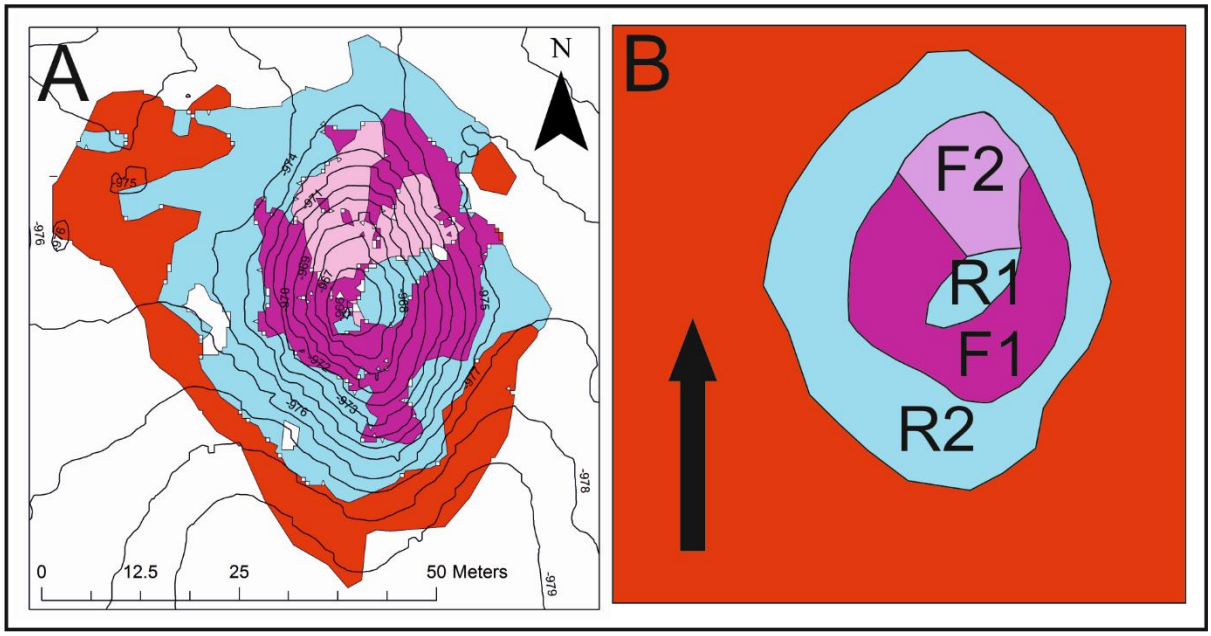

Figure 7 A) map showing the distribution of facies across Piddington Mound with 1 m contours overlaid (red = hemipelagic sediment and dropstone facies, blue = coral rubble facies, purple = dead coral framework facies, pink = live coral framework facies) B) Simplified drawing of Piddington Mound with differentiation between live and dead coral frameworks (red = hemipelagic sediment and dropstone facies, blue = coral rubble facies, purple = combined coral framework facies, R1 & R2 = coral rubble facies 2, F1 = dead coral framework facies, F2 = live coral framework facies, arrow = current direction).